Adsorption of 1,10-Phenanthroline in $HClO_4$ Solutions on Columnar-Structured Gold Electrodes. The Excluded Volume Effect

M. M. Gómez,[†] M. P. García,[†] J. San Fabián,[†] L. Vázquez,[†] R. C. Salvarezza,[‡] and A. J. Arvia*,[‡]

Departamento de Química-Física Aplicada, C-II, Facultad de Ciencias, Universidad Autónoma de Madrid, 28049 Madrid, Spain, and Instituto de Investigaciones Fisicoquímicas Teóricas y Aplicadas (INIFTA), Sucursal 4, Casilla de Correo 16, 1900 La Plata, Argentina

Received February 2, 1995. In Final Form: October 23, 1995[⊗]

The electroadsorption of 1,10-phenanthroline on columnar Au electrodes from x M 1,10-phenanthroline + 0.1 M $HClO_4$ aqueous solutions ($5 \times 10^{-4} \leq x \leq 5 \times 10^{-3}$), at constant potential and 298 K, was studied using voltammetry, chronocoulometry, and ac impedance combined with scanning tunneling microscopy to characterize the substrate topography. The roughness factor (R) was defined as the ratio of the O-adatom monolayer electrodesorption charge at the columnar Au electrode to that at the initial smooth Au electrode. When both R and the molar 1,10-phenanthroline concentration (c) were kept constant, the degree of surface coverage by 1,10-phenanthroline (θ) diminished as R was increased. The θ vs c plots, irrespective of R, were interpreted by a Frumkin adsorption isotherm including a constant standard adsorption free energy. The analysis of parameters derived from adsorption isotherms reflects the existence of an excluded volume effect, as should be expected from the 1,10-phenanthroline molecule adsorption cross section, and the size of the smallest voids and crevices at the substrate determined by scanning tunneling microscopy.

1. Introduction

For a stable solid substrate, the degree of surface coverage by a particular adsorbate present in the solution, at a constant concentration and temperature, depends primarily on the substrate−adsorbate and adsorbate−adsorbate specific interactions. It also depends on the topographic features of the substrate, which include irregularity in shape and size distribution, and adsorbate size and shape.[1] The influence of topographic features on molecular adsorption can be determined by using molecules of different adsorption cross section as yardsticks and by adequately selecting solid substrate topographies with reproducible crystallographic characteristics. It has been recently demonstrated through simulation that the heterogeneity of surface geometry is sufficient to induce adsorption/desorption hysteresis loops of different shapes according to the geometry of the surface.[2−4]

On the other hand, when electrified interfaces are considered, the applied potential also plays a role in determining the stability and configuration of adsorbates, which in turn become potential-dependent adsorbate characteristics.[2] Hence, for molecular adsorption at electrode surfaces, the use of a potential window in which the absence of faradaic reactions can be assured appears to be the most appropriate means by which to examine this complicated problem in a rather simple way.

For certain ratios of the adsorbate cross section (A) to the smallest substrate irregularity cross section (S), the influence of inaccessible substrate areas on molecular adsorption should be noticed.[1] Inaccessible substrate areas give rise to excluded volumes in a 3d-space description of the adsorbed layer. Under these circumstances, molecular adsorption measurements are equivalent to scaling the substrate surface with a yardstick of the adsorbate cross section size. Accordingly, as reported for a particular type of rough surface,[5] three limiting cases can be described (Figure 1), namely, when $A/S \rightarrow 0$, the entire substrate surface becomes accessible to the adsorbate (case 1); when $0 < A/S < \infty$, the contribution of both the excluded volume and surface fractality can be observed (case 2); when $A/S \rightarrow \infty$, the substrate roughness contribution tends to disappear as only neighboring emerging tips of the topography become accessible to molecular adsorption, i.e., the rough substrate approaches the behavior of a smooth surface defined by the highest tips of the irregular topography (case 3). In 2d-space (Figure 1), the excluded volume cross section is given by the difference between the contour of the real substrate and the contour defined by the centers of adsorbed species on the substrate.[1] It should be noted that, next to

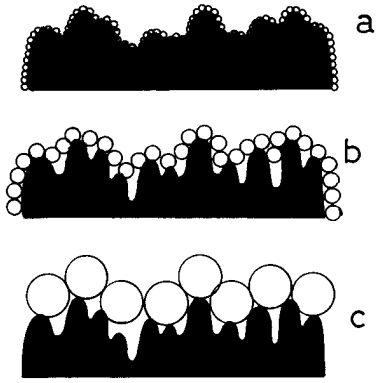

Figure 1. Two-dimensional schemes of adsorbate monolayers formed by molecules of different cross sections (white circles) on a rough surface. The ratio of the contour defined by the centers of adsorbed particles, and the surface contour itself provide information about the real adsorption surface area and the contribution of excluded areas (taken from ref 5).

[†] Universidad Autónoma de Madrid.

[‡] Instituto de Investigaciones Fisicoquímicas Teóricas y Aplicadas.

[⊗] Abstract published in *Advance ACS Abstracts,* January 15, 1996.

(1) Farin, D. and Avnir, D. In *The Fractal Approach to the Heterogeneous Chemistry*; Avnir, D., Ed.; J. Wiley, New York, 1989; p 271.

(2) Pfeifer, P.; Obert, M. In *The Fractal Approach to the Heterogeneous Chemistry*; Avnir, D., Ed.; J. Wiley, New York, 1989; p 11.

(3) Seri-Levy, A.; Avnir, D. *Langmuir* **1993**, *9*, 3067, 3073.

(4) Jaroniec, M.; Madey, R. In *Physical Adsorption on Heterogeneous Solids*; Elsevier: Amsterdam, 1988.

(5) Arvia, A. J.; Salvarezza, R. C. *Electrochim. Acta* **1994**, *39*, 1481.

0743-7463/96/2412-0818$12.00/0

inaccessibility effects, increased roughness would lead to adsorption energetic inhomogeneities because solvent−dipole interactions and adsorbate−adsorbate interactions at a certain level of roughness will start to deviate from smooth interface behavior.

The three cases described above can be approached for a number of adsorption processes which can, in principle, be followed by electrochemical methods. Thus, H-electrosorption,[6] CO adsorption,[7] CO_2 electrosorption on rough Pt,[8] the O-electrosorption on rough Pt and Au,[6] upd of Cd and Pb on Ag dendrites,[9] and the glucose electroadsorption on rough Au[10] are typical examples of case 1. In these examples, the surface roughness factor, as determined by the electroadsorption charge,[6] becomes independent of the adsorbate cross section (yardstick size) (Figure 1). In contrast, no convincing experimental data of cases 2 and 3 have been found in the electrochemical literature, except for a preliminary report where some evidence about case 2 was advanced.[5] Hence, it appears interesting to attempt to find adsorption processes at electrode surfaces which exhibit a behavior similar to the situations described for cases 2 and 3. Data resulting from those processes would allow us to establish the influence of surface irregularities on molecular adsorption isotherms and to explore the possibility of improving procedures for the evaluation of real surface area at solid electrodes.[6] For these purposes, the use of columnar-structured metal electrodes, whose topography can be quantitatively described,[11,12] appears to be the most appropriate method.

In this work, the adsorption of 1,10-phenanthroline on stabilized columnar-structured Au electrodes was investigated. The topography of these electrodes approaches that of a true rough surface consisting of columns, deep crevices, and voids,[11] as should be expected from an irregular topography without overhangs.[2] Accordingly, stabilized columnar Au electrodes can be described as self-affine surface fractals, i.e., fractals characterized by an anisotropic surface disorder. These fractals, which exhibit direction-dependent scaling properties, are characterized by a local fractal dimension (D_s) rather than the unique fractal dimension which characterizes self-similar (isotropic disordered) fractals.[1] For stabilized columnar Au electrodes $D_s \cong 2.2$.[11−13]

Results from this work show that the adsorption of 1,10-phenanthroline on these electrodes approaches the situation described above for case 2. The influence of the excluded volume on adsorption is reflected through parameters derived from adsorption isotherms resulting from these complex systems.

2. Experimental Section

Electrochemical runs were performed with a conventional cell involving columnar Au working electrodes with known roughness factors, a large area Au counter electrode, and a Hg/Hg_2SO_4 (MSE) reference electrode. All potentials given in the text are referred to the MSE scale.

The in situ preparation of columnar-structured Au electrodes by the electrochemical roughening procedure has been extensively described elsewhere.[7,14−16] Briefly, a polycrystalline Au wire immersed in 0.5 M H_2SO_4 was anodized at 2.0 V for a present time (t), at room temperature, to accumulate a certain amount of hydrous Au oxide. The oxide layer was then electroreduced by applying a linear potential sweep from 1.0 to −0.6 V at 0.1 V/s. The phase change involved in the electroreduction process occurs under a constant volume condition, i.e., the resulting columnar-structured Au layer occupies almost the same volume as that occupied by the hydrous Au oxide layer.[16,17] Then, the average thickness of the columnar-structured Au layer ($\langle h \rangle$) can be estimated from the ratio[16,17]

$$\langle h \rangle = Mq/zF\rho \qquad (1)$$

were q is the charge involved in the electroreduction of the hydrous Au oxide layer referred to the substrate area, M is the molecular weight of the Au oxide, $M = 442$ g mol^{-1}, ρ is the oxide density, $\rho = 11$ g cm^{-3}, and z is the number of electrons transferred per mole of the oxide, $z = 6$.[16,17] The validity of eq 1 was tested by scanning electron microscopy imaging of columnar-structured Au electrode cross sections.[16,17] Thus, as $q \propto t$, by adjusting t adequately, values of $\langle h \rangle$ in the range $1 \times 10^{-6} < \langle h \rangle < 1 \times 10^{-3}$ cm could be obtained.

The roughness factor (R) was voltammetrically determined from the ratio between the O-adatom monolayer electrodesorption charge at the columnar-structured Au electrode at a given t and the O-adatom monolayer electrodesorption charge at the Au electrode before the electrochemical roughening procedure was applied.[7] For this purpose, voltammograms were run in aqueous 1 M H_2SO_4 at 0.1 V s^{-1} between −0.55 and 1.15 V. No correction for the initial roughness of the Au wire was made as the value of R for the Au wire was in the range $1.0 < R < 1.1$. As already reported,[17] columnar-structured Au electrodes exhibit a surface roughness relaxation, which extends to about 1×10^5 s at room temperature, due to the relatively high mobility of Au atoms at the metal/electrolyte interface.[17] After 1×10^5 s these electrodes attain a constant value of R.[17] Thus, only columnar-structured stable Au electrodes (cs-Au), i.e. columnar-structured Au electrodes after 24 h of relaxation in 0.5 M H_2SO_4, were used.

ac impedance measurements were made using conventional circuitry at frequency $f = 160$ Hz and amplitude 7 mV.

Both voltammetric and ac impedance runs were made in aqueous 0.1 M $HClO_4$ + x M 1,10-phenanthroline ($5 \times 10^{-4} < x < 5 \times 10^{-3}$). Solutions were prepared using twice distilled water passed through a Millipore-MilliQ* system and Merck p.a. chemicals.

Voltammetric measurements to obtain the degree of surface coverage by 1,10-phenanthroline (o-ph) on Au working electrodes were made after o-ph adsorption, at a constant potential, $E = 0.1$ V, i.e., in the double layer potential range for the Au electrode in aqueous 0.1 M $HClO_4$. Saturation coverages for o-ph were obtained for adsorption times greater than 30 s. Therefore, the following adsorption conditions for o-ph on the cs-Au electrode were chosen, $E = 0.1$ V and 40 s adsorption time. All experiments were performed under purified N_2 at 298 K.

In situ scanning tunneling microscopy imaging of the stabilized cs-Au electrodes was performed in the constant current mode in 0.5 M aqueous H_2SO_4 at $E = 0.1$ V, using Nanoscope III equipment and Pt−Ir Nanotips applying 0.1 V bias voltage and 10 nA tunneling current.

3. Results and Discussion

Voltammograms obtained on stabilized cs-Au electrodes at 0.1 V/s in aqueous 0.1 M $HClO_4$, between −0.55 and 1.15 V, i.e., within the electrosorption potential range of O-containing surface species, match those obtained on smooth polycrystalline Au electrodes (Figure 2a). The

(6) Trassatti, S.; Petrii, O. A. *Pure Appl. Chem.* **1991**, *63*, 711 and references therein.
(7) Chialvo, A. C.; Triaca, W. E.; Arvia, A. J. *J. Electroanal. Chem.* **1984**, *171*, 303.
(8) Marcos, M. L.; Vara, J. M.; González Velasco, J.; Arvia, A. J. *J. Electroanal. Chem.* **1987**, *224*, 189.
(9) Hernández Creus, A.; Carro, P.; González, S.; Salvarezza, R. C.; Arvia, A. J. *J. Electrochem. Soc.* **1992**, *139*, 1064.
(10) Castro Luna, A. M.; Bolzán, A. E.; de Mele, M. F. L.; Arvia, A. J. *Z. Phys. Chem. (Munich)* **1988**, *160*, 25; *Pure Appl. Chem.* **1991**, *63*, 1599.
(11) Gómez-Rodríguez, J. M.; Vázquez, L.; Baró, A.; Salvarezza, R. C.; Vara, J. M.; Arvia, A. J. *J. Phys. Chem.* **1992**, *96*, 347.
(12) Ocón, P.; Herrasti, P.; Vázquez, L.; Salvarezza, R. C.; Vara, J. M.; Arvia, A. J. *J. Electroanal. Chem.* **1991**, *319*, 101.
(13) Gómez, M. M.; Vázquez, L.; Salvarezza, R. C.; Vara, J. M.; Arvia, A. J. *J. Electroanal. Chem.* **1991**, *317*, 125.
(14) Arvia, A. J.; Salvarezza, R. C. *Electrochim. Acta* **1992**, *37*, 2155.
(15) Chialvo, A. C.; Triaca, W. E.; Arvia, A. J. *J. Electroanal. Chem.* **1983**, *146*, 43.
(16) Vázquez, L.; Bartolomé, A.; Baró, A. M.; Alonso, C.; Salvarezza, R. C.; Arvia, A. J. *Surf. Sci.* **1989**, *215*, 171.
(17) Alonso, C.; Salvarezza, R. C.; Vara, J. M.; Arvia, A. J.; Vázquez, L.; Bartolomé, A.; Baró, A. M. *J. Electrochem. Soc.* **1990**, *137*, 2161.

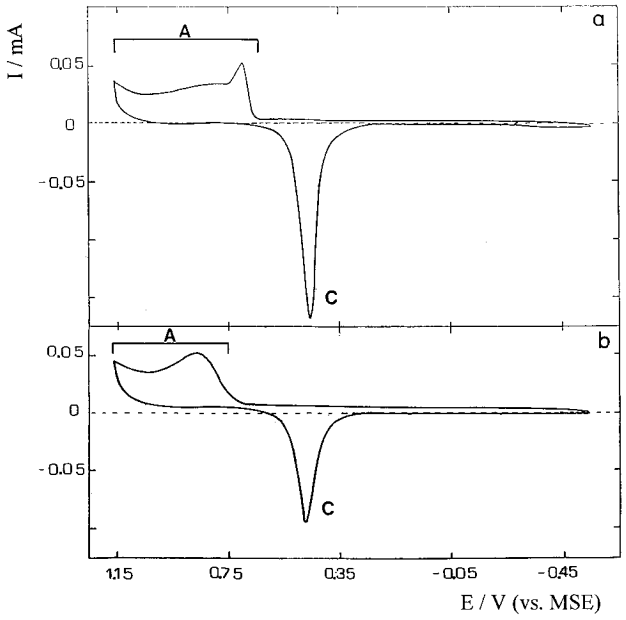

Figure 2. Voltammograms of Au electrodes ($R = 1$) in (a) 0.1 M $HClO_4$ and (b) 0.1 M $HClO_4 + 5 \times 10^{-4}$ M 1,10-phenanthroline, run at 0.1 V s^{-1} and 25 °C.

charge involved in the broad anodic current contribution extending from 0.65 to 1.15 V, labeled as A in Figure 2a, corresponds to Au oxide monolayer formation, whereas that involved in peak C belongs to the subsequent conjugated electroreduction process.[15] The charge density involved in each of these processes equates 0.40 mC cm^{-2}.[6] The hydrogen evolution reaction on Au in aqueous 0.1 M $HClO_4$ begins at potentials more negative than −0.75 V, irrespective of the type of Au electrode.

Comparable voltammograms (Figure 2b) resulting from 5×10^{-3} M o-ph + 0.1 M $HClO_4$, after holding the potential at $E = 0.1$ V for $t = 40$ s, have been reported elsewhere.[5] They exhibit a number of subtle differences as compared to those shown in Figure 2a. Thus, the presence of o-ph interferes with the formation of the O-containing surface species, as seen in the change of the initial portion of the broad anodic region A, which is shifted positively, as well as in the overall change of the voltammogram including a remarkable decrease in the voltammetric charge. Nevertheless, the magnitude of the oxidation current remains almost independent of the o-ph concentration in the solution, as has already been reported for some related compounds.[18] Therefore, it appears that in the range 0.15−1.15 V no significant faradaic process directly involving o-ph occurs. Accordingly, it seems reasonable to attribute the decrease in the charge of peaks A/C to a partial blockage of the Au electrode surface by o-ph adsorbates. After adding aqueous 0.1 M $HClO_4$ to the aqueous 0.1 M $HClO_4 + 5 \times 10^{-3}$ M o-ph solution, the charge of peaks A/C increases indicating that o-ph adsorption behaves as a reversible process.

To confirm the conclusion derived from voltammetry about the adsorption of o-ph molecules on Au electrodes with different R values, the differential capacitance was estimated at different potentials (E) in both aqueous 0.1 M $HClO_4$ and aqueous 0.1 M $HClO_4 + x$ M o-ph. To compare the behavior of Au electrodes with different values of R, the specific capacitance (C_d) was defined as the ratio between the differential capacitance and the electrode real surface area. Values of C_d in aqueous 0.1 M $HClO_4$ plotted against E (Figure 3a) for both smooth and stabilized

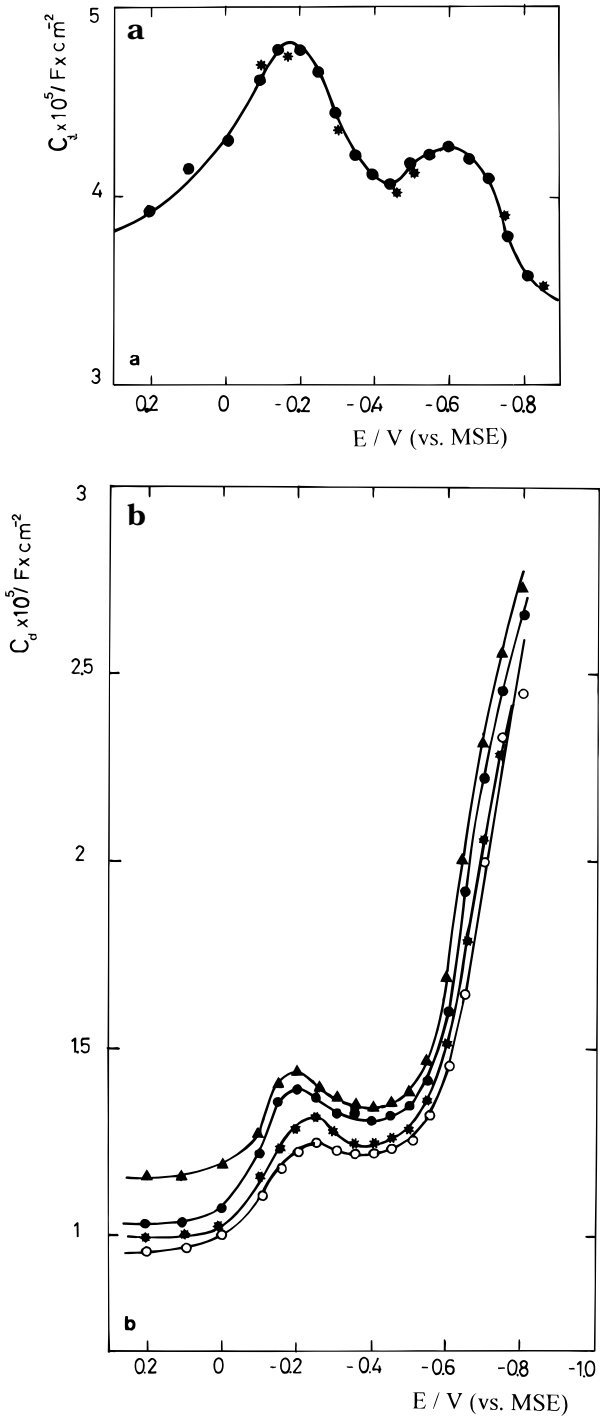

Figure 3. (a) C_d vs E plots for stabilized columnar Au electrodes in 0.1 M $HClO_4$ at 25 °C with (●) $R = 1$ and (*) $R = 33$. (b) C_d vs E plots for o-ph adsorption for $R = 33$ at different values of c: (▲) 5×10^{-4} M; (●) 7.5×10^{-4} M; (*) 1×10^{-3} M; (○) 2.5×10^{-3} M.

cs-Au electrodes appear to be fairly coincident. The shape of this plot agrees with that of plots made from data on Au electrodes in aqueous $HClO_4$ solutions.[19] The potential region around the potential of zero charge, $E_{pzc} = -0.45$ V, is dominated by the diffuse part of the double layer, whereas the rising portion, at more positive potentials, defining a maximum value of C_d at −0.2 V can be assigned to the specific structure of the inner part of the double layer.[20] Anion interactions play a dominant role on the

(18) Stolberg, L.; Richer, J.; Lipkowski, J.; Irish, D. E. *J. Electroanal. Chem.* **1986**, *207*, 213.

(19) Hamelin, A. *J. Electroanal. Chem.* **1988**, *255*, 281.
(20) Payne, R. *J. Phys. Chem.* **1966**, *70*, 204.

positive side of E_{pzc}, whereas cation interactions prevail on the negative side of E_{pzc}.

On the other hand, for a cs-Au electrode with $R = 33$ immersed in aqueous 0.1 M $HClO_4$ + x M o-ph (5×10^{-4} M < x < 5×10^{-3} M) (Figure 3b), C_d vs E plots keep essentially the same shape as in aqueous 0.1 M $HClO_4$ in the range −0.6 to −0.2 V, although C_d values are considerably diminished, as should be expected for the adsorption of organic molecules on metal electrodes.[21] Otherwise, for E < −0.6 V, the value of C_d increases markedly as E is shifted negatively. For $E = -0.75$ V, the highest cathodic potential at which no marked interference of the hydrogen evolution reaction could be observed, a value of C_d approaching that observed in aqueous 0.1 M $HClO_4$ is obtained. This fact suggests that the adsorption of o-ph on Au electrodes in the acid solution tends to be supressed as the negative charge at the electrode surface is increased. Furthermore, as the concentration of o-ph is increased, C_d vs E plots are shifted downward and the minimum in those plots and the hump at −0.2 V observed in aqueous 0.1 M $HClO_4$ tend to disappear. Therefore, results from the ac impedance data confirm that for E > −0.6 V, o-ph is adsorbed on Au electrodes, as suggested by voltammetric data.

The value of θ, the degree of Au surface coverage by o-ph, can be estimated from the decrease in Q_c, the O-electrodesorption voltammetric charge, as compared to the value resulting from aqueous 0.1 M $HClO_4$. For this purpose, θ is defined by $\theta = 1 - (Q_c^*/Q_c)$, where Q_c and Q_c^* are the electroreduction charge before and after o-ph adsorption, respectively. Similar values of θ were obtained using Q_a and Q_a^*, the charge of anodic peak A before and after o-ph adsorption, respectively. Values of θ determined by an indirect method such as voltammetry were confirmed by chronocoulometry.[22] In this case, the values of $q(E)$, the charge density at a given potential (E), were determined by integration of potentiostatic current transients in the supporting electrolyte (q_1) and in the supporting electrolyte containing o-ph (q_2). The value of Δq, the change in the charge density due to the o-ph adsorption, is $\Delta q = (q_1 - q_2)$. The value of q^M, the absolute value of q in the presence of o-ph, was then calculated by adding Δq to the value of q calculated by integration of the capacity curve measured in the supporting electrolyte alone. Comparative q^M vs E plots obtained for the Au electrode with $R = 1$ in aqueous 0.1 M $HClO_4$ + x M o-ph (Figure 4) show that as c is increased the value of q^M increases although all curves intersect at $E_{ad}^M = -0.05$ V, the potential of maximum adsorption.

For values of E comprised in the range between E_{ad}^M and $E_{pzc} = -0.45$ V, the value of q^M exceeds that resulting from 0.1 M $HClO_4$, but it diminishes as $E \rightarrow E_{pzc}$. When E < E_{pzc}, the value of q^M gradually approaches that observed in 0.1 M $HClO_4$. These facts can be taken as an indication that the adsorption of o-ph occurs on a positively charged Au surface at a flat position favored by an interaction of π-orbitals of the o-ph molecule with the positively charged Au surface,[21] as has been found for the adsorption of aromatic compounds on Au[22] and Pt[23] in acidic and neutral media. Accordingly, the interaction between π-electrons of the o-ph molecule and the Au surface becomes gradually weaker as E is negatively

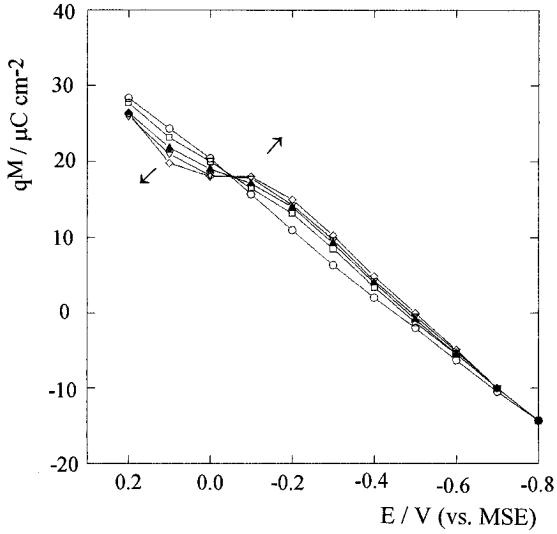

Figure 4. q^M vs E plot: (○) 0.1 M $HClO_4$; (□) 0.1 M $HClO_4$ + 5×10^{-4} M o-ph, (▲) + 7.5×10^{-4} M o-ph, (▼) + 2.5×10^{-3} M o-ph, (◇) + 5×10^{-3} M o-ph. Arrows indicate the increasing o-ph concentration.

Table 1. Values of θ for Different o-ph Concentrations Determined by Voltammetry and Chronocoulometry at a Au Electrode (R = 1) and 298 K

	θ	
c, M	voltammetry	chronocoulometry
5×10^{-3}	0.31	0.35
2.5×10^{-3}	0.28	0.30
1×10^{-3}	0.26	0.28
7.5×10^{-4}	0.24	0.24
5×10^{-4}	0.21	0.22

displaced. When E < E_{pzc} repulsive adsorbate−substrate interactions should prevail. This interpretation is consistent with the large increase in C_d as the electrode surface is negatively charged (Figure 3b).

On the other hand, for E > E_{ad}^M the value of q^M lies below that resulting from 0.1 M $HClO_4$ due to the competitive adsorption interaction among o-ph and other constituents of the solution, mainly water,[24] i.e., the organic molecule interferes with the formation of adsorbed OH species on Au. This interference becomes more remarkable as c is increased.

The q^M vs E plots were integrated to give γ, the surface tension, and from the γ vs ln c plots the value of θ was estimated (Table 1). Values of θ, obtained by the indirect voltammetric method involving the blockage of Au oxide formation, are in good agreement with those derived from chronocoulometry. Therefore, the voltammetric method is adequate to estimate θ for the o-ph adsorption on Au electrodes.

The θ vs c plots (adsorption isotherms) for cs-Au electrodes ($1 \leq R \leq 55$) are displaced toward lower values of θ as R is increased (Figure 5). Although these plots show a similar shape, they are clearly shifted in the direction expected for a decreasing θ when R is changed from 1 to 55. The adsorption isotherms shown in Figure 5 can be fitted by a Frumkin-type isotherm[25,26]

$$\beta x = \theta \exp(-2a\theta)/(1 - \theta) \qquad (2)$$

where x is the molar fraction (c/c_s), a is a complex

(21) Gileadi, E. *Electrosorption*; Plenum Press: New York, 1967. Damaskin, B. B.; Petrii, O. A.; Batrakov, V. V. *Adsorption of Organic Compounds on Electrodes*; Plenum Press: New York, 1971. Damaskin, B. B.; Kazarinov, V. E. In *Comprehensive Treatise of Electrochemistry*; Bockris, J. O'M., Conway, B. E., Yeager, E., Eds.; Plenum Press: New York, 1980; Vol. 1, Chapter 8, p 353 and references therein.

(22) Nguyen Van Houng, C. *J. Electroanal. Chem.* **1983**, *264*, 247.

(23) Albalat, R.; Claret, J.; Feliu, J. M.; Clavilier, J. *J. Electroanal. Chem.* **1990**, *288*, 277.

(24) Ferro, C. M.; Calandra, A. J.; Arvia, A. J. *J. Electroanal. Chem.* **1975**, *59*, 239.

(25) Lipowski, J.; Nguyen Van Huong, C.; Hinnen, C.; Parsons, R.; Chevalet, J. *J. Electroanal. Chem.* **1983**, *143*, 375.

(26) Parsons, R.; Peat, R. *J. Electroanal. Chem.* **1981**, *122*, 299.

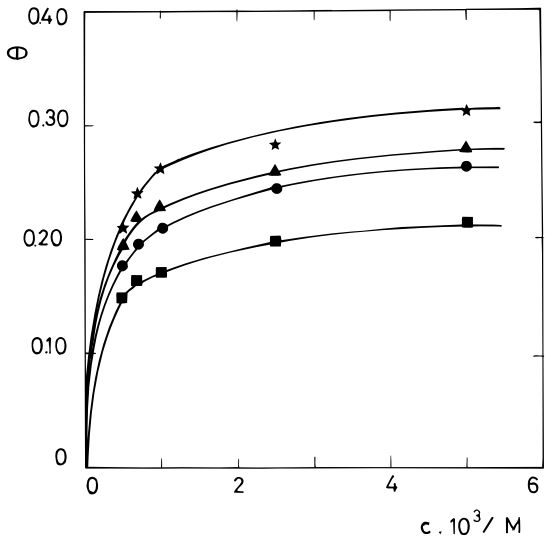

Figure 5. θ vs c plots for 1,10-phenanthroline adsorption in 0.1 M $HClO_4$ at 25 °C on columnar Au electrodes with different values of R at a constant potential, $E = 0.1$ V: (*) $R = 1$; (▲) $R = 16$; (●) $R = 32$; (■) $R = 55$. Solid lines correspond to the theoretical plots calculated using eqs 2 and 3 and values of a and $\Delta G°$ assembled in Table 1.

Table 2. Values of a and $\Delta G°$ Derived from Equations 2 and 3 and Data Shown in Figure 5

R	a	$\Delta G°$/kJ mol^{-1}
1	−11.1	−35.7
16	−12.2	−35.9
33	−12.7	−34.0
55	−16.2	−35.5

interaction parameter, and β is the adsorption coefficient given by

$$\ln(\beta/c_s) = \Delta G°/RT \qquad (3)$$

where c_s is the solvent concentration ($c_s = 55.5$ M), $\Delta G°$ is the standard free energy of adsorption, T is the absolute temperature, and R is the universal gas constant. Experimental data can be fitted with eq 2 by using the values of a and $\Delta G°$ assembled in Table 2. The value $\Delta G° \cong -35$ kJ mol^{-1} is close to those reported for the adsorption of aromatic compounds on noble metals[21] and somewhat higher than those found for the adsorption of several anions on platinum.[27] Hence, the value of $\Delta G°$ is consistent with the fact that the o-ph molecule remains adsorbed at the early stages of the O-containing surface layer formation, leading to a partial blockage of the electrode surface for water molecule electroadsorption.

As R is increased, the value of a decreases but the value of $\Delta G°$ is almost constant. A constant value of $\Delta G°$ is expected for a substrate involving crystallographic features which are substantially independent of roughness. For instance, it has been well established that for pyridine adsorption on gold[28] the value of $\Delta G°$ displays a strong dependence on surface crystallography. The constant value of $\Delta G°$ is therefore consistent with voltammetry data which exhibit no current peak change that can be attributed to changes in the distribution of surface crystallography as R is increased. In principle, the value $\Delta G° \cong -35$ kJ mol^{-1} would then indicate a weak adsorbate/substrate interaction, and the negative sign of a would correspond to a repulsive interaction among adsorbed molecules.

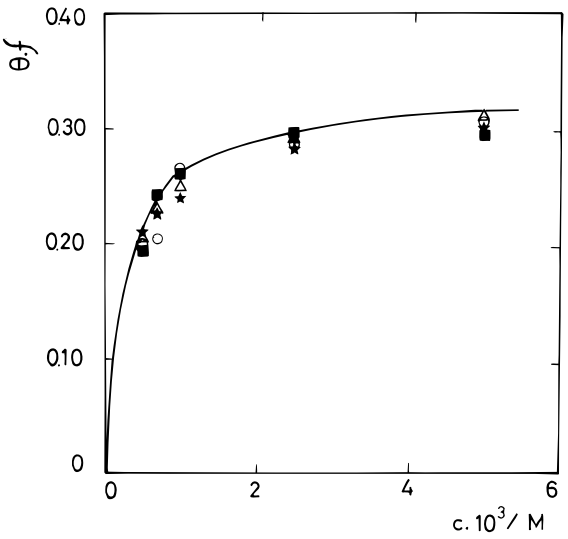

Figure 6. θf vs c plot: (△) $f = 1$ ($R = 1$); (■) $f = 1.10$ ($R = 16$); (☆) $f = 1.18$ ($R = 33$); (○) $f = 1.4$ ($R = 55$). The solid line corresponds to the theoretical plot calculated using eqs 2 and 3 and values of a and $\Delta G°$ for $R = 1$ (Table 1), 25 °C.

Neglecting any surface roughness correction to the adsorption isotherm, it would be possible to interpret Frumkin lateral interaction parameters (Table 1) in terms of free enthalpy changes.[29] However, in the present case, despite the fact that adsorbed 1,10-phenanthroline may well be a cation in acid solutions, seemingly there is no specific reason to expect an increase in the repulsive interaction as the electrode surface becomes rougher.

Let us consider then the possibility that for the type of substrate used in this work the values of a and β incorporate mainly the influence of surface topography on the adsorption isotherm. A strong support to this view is that the θ vs c plots can be easily normalized just by taking into account f, a surface roughness-dependent correction factor (Figure 6). This factor is an adjustable parameter that takes the value needed to bring all the adsorption isotherms together, irrespective of the value of R. Its value is chosen in such a way that by plotting (θf) vs c, all isotherms fall on a single curve leading to values of a and β coinciding with those derived for $R = 1$ (Table 2). This would mean that the surface topography no longer influences the values of a and β, and hence, the physical meaning of a and β in the Frumkin isotherm is kept. Correspondingly, the value of $(1 - f^{-1})$ can be assigned to the fraction of surface sites lost as active adsorption sites for a particular adsorbent, i.e., f reflects the presence of excluded areas (in two dimensions) or volumes (in three dimensions) in the substrate. The value of $(1 - f^{-1})$ increases linearly with R (Figure 7).

The presence of excluded volumes in the rough substrate topography can be related to both the size of surface irregularities at cs-Au electrodes and the size of the o-ph molecule itself. The o-ph molecule cross section calculated using the MM2 method[30] is close to 10^{-14} cm^2. This figure can be considered as the area occupied by each adsorbate on the substrate. Therefore, the o-ph cross section would establish a size limit for the full accessibility of voids and crevices at the cs-Au electrodes to o-ph adsorption. In fact, low-magnification STM images of stabilized cs-Au electrodes show crevices and voids with sizes larger than the molecular cross section, whereas high-resolution STM

(27) Molina, F. V.; Posadas, D. *Electrochim. Acta* **1988**, *33*, 661.
(28) Lipkowski, J.; Stolberg, L.; Yang, D. F.; Pettinger, B.; Mirwald, S.; Henglein, F.; Kolb, D. M. *Electrochim. Acta* **1994**, *39*, 1045.
(29) van Leeuwen, H. P.; Lyklema, J. In *Modern Aspects of Electrochemistry*; Bockris, J. O'M., Conway, B. E., White, R. E., Eds.; Vol. 17, Ch. 6, p. 411, Plenum Press: New York, 1986; Vol. 17 Chapter 6, p 411 and references therein.
(30) Allinger, N. L. *J. Am. Chem. Soc.* **1977**, *99*, 8127.

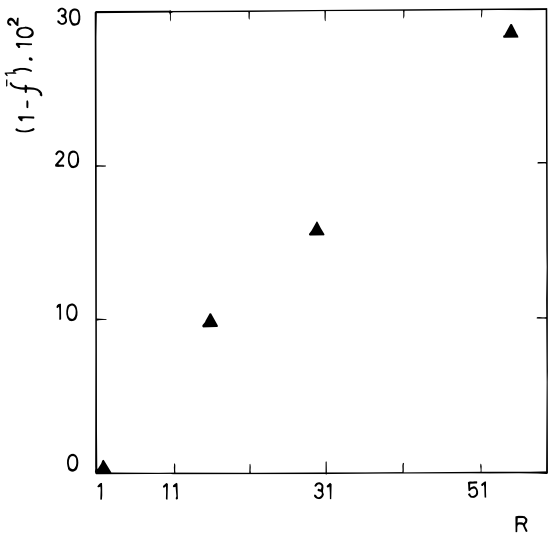

Figure 7. $(1 - f^{-1}) \times 100$ vs R plot for the 1,10-phenanthroline adsorption in 0.1 M $HClO_4$ on columnar Au electrodes, 25 °C.

images (Figure 8a,b) reveal that a fraction of the cs-Au electrode is made of small voids and crevices with a cross section area of about $(1-2) \times 10^{-14}$ cm^2. This is clearly seen from the analysis of the image cross sections (Figure 8c−e). The void profiles, indicated by arrows in Figure 8c−e, exhibit a width and a depth close to 10^{-7} nm, a size which is comparable to the cross section of the o-ph molecule adsorbed parallel to the substrate surface. It should be noted, however, that there is an intrinsic limitation on determining the smallest void and crevice dimensions by STM owing to the finite size of the tip itself (Figure 8f).[31] Therefore, the presence of smaller features (in size) and larger features (in depth) than those shown in Figure 9 cannot be a priori excluded. Therefore, considering the irregularity size distribution, it is feasible that the smallest voids become inaccessible to the o-ph molecule. Thus, the o-ph adsorption on these substrates implies the appearance of the excluded volume effect. It should be noted that attempts to image the o-ph molecule were unsuccessful owing the rough topography of the cs-Au electrodes.

It should be noted that for the electrochemical system, Au atoms at the excluded volumes are in contact with the supporting electrolyte in the nanometer-size environments created by the o-ph molecule adsorption. These Au atoms are able to electro-oxidize when an adequate anodic potential is applied to the electrode. The voltammetric charges involved in peaks A−C in Figure 1b reflect both the number of Au atoms as o-ph-free Au atoms and those Au atoms lying in the nanometer-size environments created at the excluded regions.

The above explanation is consistent with a number of facts already reported for this type of electrode. Thus, in contrast to the adsorption characteristics of o-ph on cs-Au electrodes, no excluded volume effects were detected on the same type of electrode for CO_2[8] and glucose[10] electroadsorption, as should result from these adsorbates because the ratio $A/S \Rightarrow 0$. The same interpretation applies to CO adsorption data on cs-Pt columnar structured electrodes.[32]

The preceding interpretation based on an excluded volume effect was confirmed by studying the adsorption on the same substrates of thymol blue, a molecule with an average molecular cross section larger than that of o-ph. The adsorption of thymol blue involves different

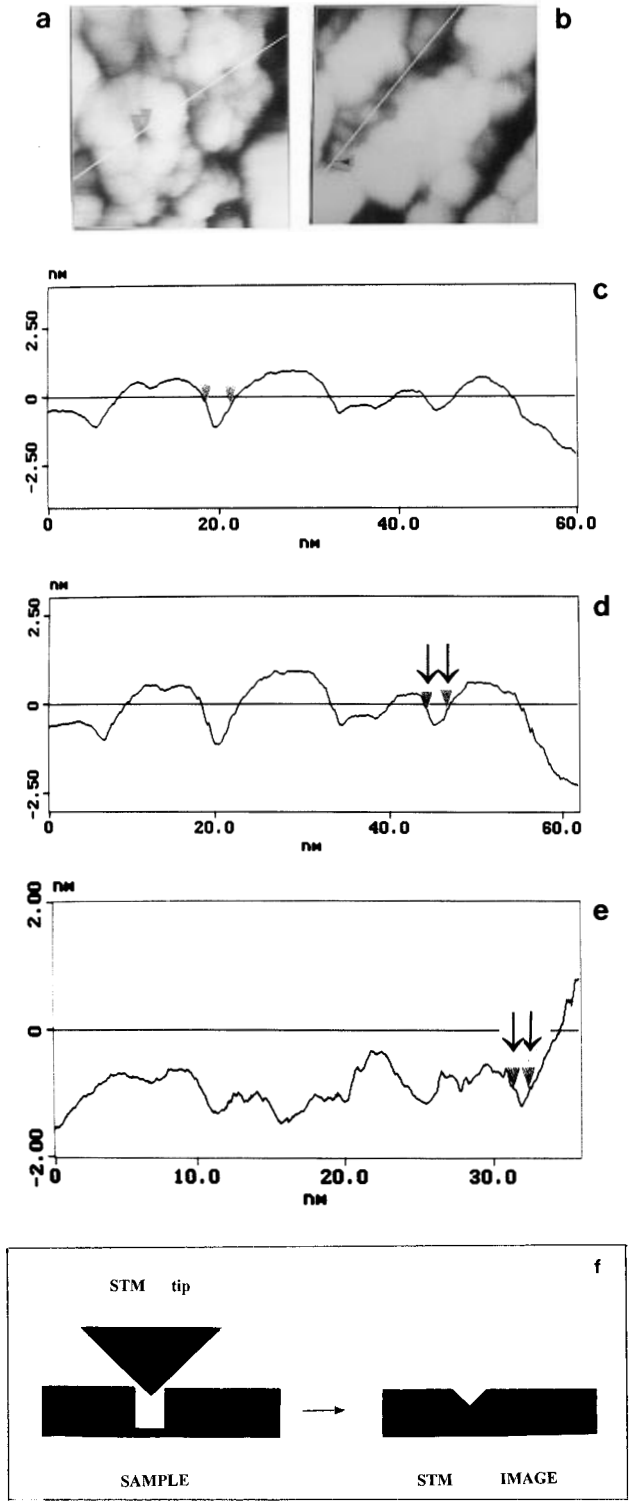

Figure 8. In situ 50 × 50 nm^2 (a) and 34 × 34 nm^2 (b) STM images and cross sections (c−e) of a cs-Au electrode ($R = 30$). Arrows indicate voids among columns with a size in the order of 10^{-7} cm. Images were taken at $E = 0.1$ V in 0.5 M H_2SO_4 after cs-Au electrode stabilization. (f) Scheme showing the possible influence of the tip size on void and crevice imaging by STM.

possible adsorbate configurations with approximate cross sections lying in the range 1.2×10^{-14} to 1.5×10^{-14} cm^2. In this case, adsorbate surface coverages referred to the original substrate surface area determined by the O-atom electroadsorption are considerably decreased (Table 3) with respect to those obtained for o-ph adsorbates, in agreement with the preceding interpretation.

(31) Topometrix Corp. *Artifacts in SPM*; Santa Barbara, CA, 1994.
(32) Bilmes, S. A.; Arvia, A. J. *J. Electroanal. Chem.* **1993**, *361*, 159.

Table 3. Values of θ for the Adsorption of Thymol Blue at Different Concentrations on Au Electrodes with Different Values of R in 0.1 M $HClO_4$ Solution at 298 K

	θ	
c, M	$R = 1$	$R = 33$
1.0×10^{-5}	0.09	0.02
2.5×10^{-5}	0.15	0.04
5.0×10^{-5}	0.20	0.06
7.5×10^{-5}	0.22	0.06

From the results of this work, it can be, therefore, concluded that for molecules (yardsticks) with effective adsorption cross sections larger than or in the order of the smallest irregularities at the substrate, i.e., $0 \leq A/S \leq \infty$, a fraction of the substrate area always becomes inaccessible to the adsorbate, leading to a decrease in the available adsorption area which reflects in the behavior of the adsorption isotherms.

Acknowledgment. Financial support was obtained through projects PS88-0014 (DGICYT-Spain). R.C.S. and A.J.A. thank CONICET (Argentina) and the Universidad Autónoma de Madrid for their participation in this research project.

LA950079Z